ISSN: 2639-7455

Research Article

Earth & Environmental Science Research & Reviews

Impacts on Estuarine Ecosystem from Climate Changes Based on Modeling Experiments within Delaware Bay

Zhiren Wang

Institute of Marine and Coastal Sciences, Rutgers, The State University of New Jersey

***Corresponding author**
Zhiren Wang, Institute of Marine and Coastal Sciences, Rutgers, The State University of New Jersey, 71 Dudley Road, New Brunswick, NJ 08901; Email: joewwh77@gmail.com

Submitted: 10 Jan 2019; **Accepted**: 17 Jan 2019; **Published**: 06 Mar 2019

Abstract

Coastal regions concentrate ecological behaviors, have more observations, permit high-resolution modeling, and serve as a good climate-changing sensor. For the Delaware Bay, a high-resolution hydro-dynamical model (ROMS) was tailored, validated and applied to hindcast its largely unrecorded physical environment, to investigate the roles of the physical environment influencing oyster diseases, and to inquire into the future fate of the bay in response to climate changes. Sensitivity studies suggested that 50-100-cm sea-level rise (SLR) in approximately 50-100 years may occur and salinize the Delaware Bay mainly through weakening salinity gradient and salt advection due to the intensified mixing induced by the widened bay. Highly correlating to mixing and therefore changing salt advection, the width of the bay mattered to salt intrusion distance more than the depth of the bay did. This conclusion is differenet than that from the classic theories that emphasize the depth in influencing the salt intrusion distance via the steady shear dispersion. The SLR-induced salinization may not be offset by intensified river flow input, but may be substantially mitigated by fixing the coastline (or width). Climate warming may warm the shallow and thermally sensitive bay. The warm and salty conditions would compromise freshwater resource in the upper bay and be generally unfavorable to oysters by promoting oyster diseases (i.e., MSX and Dermo). Salinization might occur in other similar estuaries of narrow geometry, shallow depth, and small volume.

Keywords: Estuary salinization, physical environment, sea-level rise, climate warming, oyster diseases, Delaware Bay

1. Introduction

Delaware Bay functions as a producer of organic matters, a protective habitat for aquatic life and wildlife, a freshwater provider, and a good climate-changing sensor with sensitive responses to climate variability. As one of the ecological members within Delaware Bay, oysters (*Crassostrea virginica*) live along salinity gradients and are sensitive to their physical environment. Oyster population abundance within Delaware Bay was high during 1970-1985, but low during 1953-1969 and 1985-1999, and very low since 2000. Oyster population abundance is closely related to environmental fluctuations, harvest and recruits and oyster mortality. The mortality of oysters is controlled under two lethal diseases: Multinucleated Sphere of unknown origin (MSX) and Dermo. The recorded outbreaks of the MSX were in 1957 and 1985 within Delaware Bay, killing many oysters [1-3]. The majority of the oyster population has developed a relatively high level of resistance after approximately 1990s with the significantly decreased MSX prevalence (MSXP). Laboratory studies show that salinity and temperature are the primary physical controls on MSX, with MSX requiring salinities higher than 10psu and temperatures of approximately 5-20°C. Infection prevalence generally decreases along a salinity gradient with salinities. Infection prevalence can be eliminated from oysters at salinity lower than 10psu, which provides a disease refuge, but high salinity does not always guarantee high MSXP levels, nor does low salinity always prevent the parasite from appearing in the upper bay. The gradient of infective particles from lower to upper bay exists and provides a disease-transport mechanism through circulations [4, 5]. Oyster parasites are relatively inactive at 5°C and below, but multiply faster than the oysters can control between approximately 5°C and 20°C [6-8]. Both MSX and Dermo multiply fast at higher temperature (above 18-20°C) and salinity higher than approximately 12psu [2, 9].

The field circulations, salinity, and temperatures within Delaware Bay must have been influencing the ecosystem of Delaware Bay in a comprehensive way and are controlled, e.g., fundamentally by tides, river flow inputs, and atmospheric forcing. Tides provide energy for mixing and induce strong currents (~5 m/s), with principle lunar (M_2, with a period of 12.42 hours and the most dominant amplitude), principle solar (S_2, 12.00 hours), and larger lunar elliptic (N_2, 12.66 hours) as the major tidal constituents to produce spring and neap variability at 14.8 and 27.3 days, respectively [10]. An inter-play between river input, exchange flow, and mixing determine the estuarine structure of current shear and the along-channel salinity gradient [11-17]. The primary measure of the highly variable salinity structure is salt-intrusion distance, the distance from the estuary mouth to the point where the salinity reaches the river salinity [18]. Atmospheric forcing influences circulations and temperatures of the bay through winds and heat fluxes associated with climate background. Climate background can provide a bridge between water

temperatures and salinity and produce a negative correlation between water temperatures and salinity within Delaware Bay. Heat fluxes determine air and water temperatures. Warmer atmosphere enhances precipitations and snow-ice melting and therefore hydrological conditions, and hydrological conditions change salinity [19].

However, the physical environment of Delaware Bay has gone largely unrecorded and, and questions still remain pertaining the relationship between the physical environment and oyster disease. The physical environment needs to be "reconstructed" through modeling by applying more realistic control equations and observed data that serve as forcing, initial and boundary conditions. Modeling and correlation studies are performed in Wang et al. [5] and shows that salinity and temperature influence MSX prevalence (MSXP), and are out of phase under a regular climate background where river flow increases with warmer air (therefore corresponding with higher water temperatures) through enhanced precipitations or snow-ice melting and the increased river flow input decreasing salinity, which has helped control the MSXP. However, concurrent warmer and saltier conditions did occur within Delaware Bay under an "irregular" climate background, e.g., during the persistently drier and warmer period of 1984-85 when MSXP was high, following the unusually strong El Niño in 1982-83 [5, 20]. Warmer and saltier conditions can also be induced by global warming and less river flow input due to reduced precipitations or snow-ice melting. In other words, the favorable physical environment of Delaware Bay may be compromised by climate changes in temperatures and hydrological conditions.

Climate is changing and climate changes must be considered in determining the physical environment for Delaware Bay. During 1906-2005/1956-2005, the global mean surface temperature has risen by 0.07±0.02/0.13±0.03°C per decade, and has been further enhanced since approximately 1994 [21]. By 2070-2099 with a CO_2 level of approximately 850 ppm for a medium-high emission, a 4.9 ±1.8°C increment of the sea surface air temperature over Delaware Bay has been predicted by global climate models [22]. As a result of the warming, global average sea level has risen at a rate of approximately 1.8±0.3 mm/yr over the second half of the 20th century [23, 24]. Model-based studies predict that sea-level within Delaware Bay could rise by 40 to 65 cm by 2100 due to climate warming [25]. Another consequence of warming is the reduction of snow and ice coverage. River discharge changes with sea ice extent that has shrunk since 1978 by approximately 2.7 ± 0.6% per decade and with precipitation that has generally increased over land north of 30°N during the period from 1900 to 2005 [19, 26, 27].

Climate changes will directly influence the environmental conditions and therefore oyster diseases within Delaware Bay. How might the evolving climate over the next 50 to 100 years influence the salinity and temperature fields within Delaware Bay? Specifically: Is the Bay likely to become more saline, by how much, and which climate changes will be most influential? How might the salinity structure, e.g., salt wedge, change with time? How might the response of salinity to freshwater input be modified? How much warmer might the shallow and thermally sensitive bay get in response to the higher surface air temperature associated with global warming? How might the distribution and occurrence of salty-warm water change, and what might be the implications for the conditions at the locations of present-day oyster beds? To answer these questions, climate sensitivity studies were conducted in Section 2. Experimental results on temperature and salinity were presented in Section 3. The potential impacts of the new physical condition on oyster abundance were analyzed in Section 4, followed with theoretical consideration in Section 5 and summary in Section 6.

2. Numerical experiments conducted for climate sensitivity studies

Two sets of experiments were conducts to perform a series of climate sensitivity studies, as described below and in Table 1. The standard experiments with thirteen cases used the same minimum water depth of 2 meters as the validated model performed in Wang et al. [5]. The diagnostic experiments with five cases used varying minimum water depths of 0.25 and 2 meters, wet-dry geometry, enlarged geometry, and different initial salinity to examine and enhance the results from the standard experiments for SLR2.

The years 2000-02, the beginning of the 21st century between La Niña and El Niño phases during an ENSO cycle, were set as the normal case (Norm). Based on the Norm, cases for climate warming, SLR and hydrology change were designed, as described in follows:

Case Warm was conducted with a surface air warming of 5 °C (relative to 2000-2002).

Sea level rose and has risen faster recently (1981-2011), coinciding with the warmest years on record since 1850 during 1995-2006. During this interval, mean sea level within Delaware Bay increased by approximately 5.01 mm/yr (Figure1A). In 50-100 years, sea level can rise by 50 to 100 cm. Experiments for the 50-cm and 100-cm SLRs (cases SLR1 and SLR2) were performed in order to examine the influence of widened geometry and deepened bathymetry induced by SLRs; while SLR3, a companion experiment to case SLR1 but with the coastline fixed, was run to assess the effect of the horizontally enlarged geometry.

Global warming will likewise alter the atmospheric circulation. On average, the cross-bay/along-bay wind component increased/decreased by approximately 100%/-27.7% (relative to the standard deviation of cross-bay/along-bay wind component) per century within the period of 1981-2011 (Figure1B). Changes in the amplitude and direction of wind could change the circulation and shear within Delaware Bay through alterations in wind-driven currents, Ekman transport, and mixing. Wind1 and Wind2 were designed to examine the effects due to changing cross-bay and along-bay winds, with consideration that the general circulation changes more in direction than in size during the major inter-annual variations [20].

Over the period 1981 to 2011, the river discharge input into Delaware Bay had an increasing rate of 6.83 $m^3/s/yr$ (Figure 1C), larger than the increasing rate of approximately 0.59 $m^3/s/yr$, within the period of 1913-2011 (USGS data of the Delaware River at Trenton, figure omitted). A relative change in river discharge during each month (prepared by Pollard, pollard@essc.psu.edu) displayed a significant summer and autumn increase in river discharge (RD1 in Figure 1D). However, earlier predictions yielded a decreased annual stream flow, -39 to 9%, over the Delaware River Basin between 2070-2099, with a doubled CO_2 level [28]. Using these data as a reference, three numerical experiments (RD1, RD2 and RD3, Figure 1D) were conducted in order to examine the effects from predicted (+20-200% from April to November), higher (+50% in spring), and lower (-50% in spring) river discharge, respectively.

The SLR1, SLR2, Warm, and RD1 are of high likelihood to occur for the future. Experiments Comb1 (SLR1+Warm+RD1), Comb2 (SLR2+Warm+RD1), and Comb3 (SLR3+Warm+RD1) were conducted to examine their comprehensive effects.

To ensure that the results from SLR1 and SLR2 were convincing, five diagnostic experiments were performed, as follows: SLR2I to determine whether or not a fresher initial condition may eventually reduce the salinity in SLR2 by removing the salt in the new water area induced by SLR2 from the initial conditions of SLR2; SLR2W to determine the effect from only a widened geometry by keeping the normal bathymetry intact but using the same land-sea mask as SLR2 (the bay was enlarged in the same manner as SLR2, but there was no SLR-effect on water depth); and NormWD, SLR2WD, and Comb2WD, same as Norm, SLR2 and Comb2 respectively, but using a wet-dry scheme, 25cm minimum water depth, and running through for three years with a much smaller time step (15 seconds) and with coastal lines changing with sea levels and time.

The model was run for three years for each of the cases. One year was set aside for model adjustment. Case SLR1 adjusts the slowest and reaches an equilibrium state after approximately eight months. Therefore, one year was sufficient for model adjustment.

In the following text, the first year was simply called the adjustment phase, while the second year, when modeling reached an equilibrium state, was referred to as the equilibrium phase (the modeling during the third year made little difference to the analysis but was performed).

The experiment results for all the cases were relative to case Norm, expressed with the departures from the Norm for salinity, temperature, currents, and salty-warm water area (SWA), an area of the bottom water whose temperature/salinity is higher than 17.5°C/12.5psu [5]. Positive vertical difference (PVD) was used to scale the stratification of salinity (bottom minus surface), temperature (surface minus bottom), and the shear of currents (surface minus bottom). Thus, positive/negative PVD indicated an enhanced/weakened stratification or shear

Table 1: Standard and diagnostic experimental cases: The departures from the Norm were listed for ESI (%, Eq.4), salinity (psu), temperature (°C) and currents averaged within one year after the model runs through the first year for full adjustment. The numbers in row "Norm" represent mean values.

Standard experiments with 2 m minimum water depth								
Case	**Definition**	**ESI**	**Salinity**		**Temperature**		**Current**	
			BO T	**PVD**	**BOT**	**PVD**	**SUR**	**PVD**
Norm	Normal case in 2000-2002	0	17.9	0.6	13.3	0.3	10.0	6.7
SLR1	1-m SLR	+24	+8.2	-0.6	+0.4	-0.2	-3.9	-3.1
SLR2	0.5-m SLR	23	+8.0	-0.6	+0.5	-0.2	-4.2	-3.3
SLR3	1-m SLR with coast-line fixed	+7	+1.7	+0.1	-0.2	+0.1	+0.9	+0.7
Warm	5°C-warmer surface air	+1	+0.3	+.03	+3.0	+0.1	+.03	+0.1
RD1	Predicted river flow + 20–200%	-8	-1.6	+0.3	-0.1	+0.1	+1.3	+0.9
RD2	MAM river flow + 50%	-2	-0.3	+.08	-.04	+.02	+0.4	+0.2
RD3	MAM river flow -50%	+3	+0.5	-0.1	+0.1	-.03	-0.5	-0.3
Wind1	Cross/along-bay wind +/-30%	-4	-0.7	-.01	+0.3	-.04	-0.3	-0.2
Wind2	Cross/along-bay wind -/+30%	+3	+0.7	-.00	-0.2	+.01	+0.4	+0.2
Comb1	SLR1+Warm+RD1	+22	+7.5	-0.6	+3.6	-0.2	-3.7	-3.0
Comb2	SLR2+Warm+RD1	+21	+7.3	-0.6	+3.6	-0.2	-4.0	-3.1
Comb3	SLR3+Warm+RD1	+4	+0.6	+0.5	+2.6	+0.3	+2.5	+2.0
Diagnostic experiments to exam results from Standard experiment SLR2								
SLR2I	SLR2 but zero initial salinity for new water to check fresher initial conditions							
SLR2W	SLR2 but zero SLR to check a purely widened geometry							
NormWD	Same as Norm but using a wet-dry scheme and 25cm minimum water depth							
SLR2WD	Same as SLR2 but using a wet-dry scheme and 25cm minimum water depth							
Comb2WD	Same as Comb2 but using a wet-dry scheme and 25cm minimum water depth							

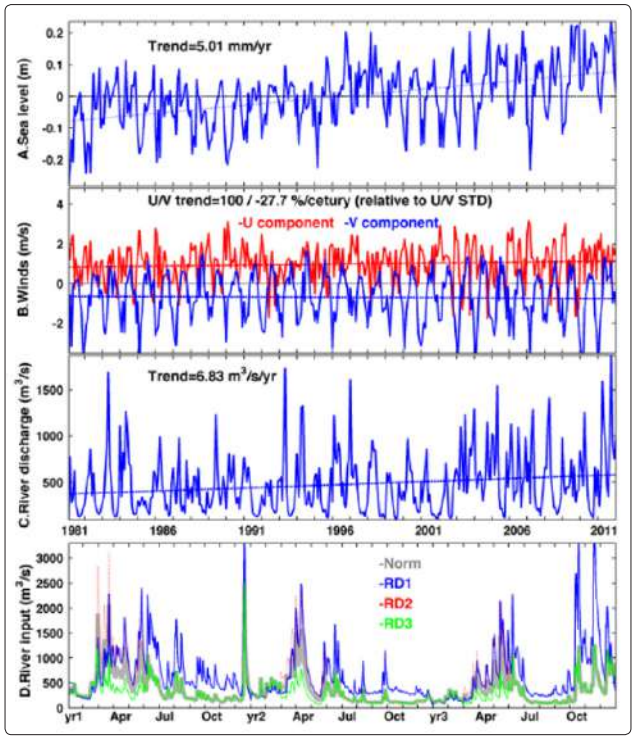

Figure 1: A. Mean sea-level height of Delaware Bay (data are from the National Water Level Program). **B**. The cross-/along-bay winds (named the U/V component, m/s, and red/blue lines) 10 m above the sea surface (data are from the North American Regional Reanalysis). C. The river flow (m^3/s) input into Delaware Bay (data are from the U.S. Geological Survey). **D**. The modeling river flow (m^3/s) input into Delaware Bay under modern (gray: Norm) and predicted future (blue: RD1, Pollard, pollard@essc.psu.edu) conditions, as well as the 50% increment/reduction during March-May of modern river flow (red/green, RD2/RD3, as described in Table 1).

3. Experimental Results

The experimental results were analyzed in Table 1, Figure 2, Figure 3, and Figure 4 for the standard cases. The salinity departures from case Norm for cases SLR2, SLRI and SLR2W, and from case NormWD for cases SLR2WD and Comb2WD were depicted in Figure 5, based on the salinity averaged within entire Delaware Bay. The RD2, RD3, Wind1, and Wind2 produced minor effects on temperature, salinity, and SWA, with their results simply listed in Table 1 and plotted in Figure 2 and Figure 6. The significant effects were described below.

Experimental results on temperature and its PVD

The Warm increased the water temperatures of the shallow and thermally sensitive bay by ~1 to 3°C, with ~10-20W/m^2 more sensible heat flux inputting into the bay and increased temperature PVD by ~0.3 °C. The SLR2 (SLR1 similar) warmed the bay by ~0.5 to 1.0 °C (~0.4 °C totally, ~0.5 to 1.2 °C in spring and summer, but ~ -0.2 °C in winter and fall), weakened the temperature PVD up to -2°C in summer, and enhanced the mixing (see Section 5 for details). The Comb2 (Comb1 similarly) amplified the warming effect with bottom temperature increasing up to 4 °C (as compared to the Warm or SLR2), weakened temperature PVD up to -2 °C in summer (similar to case SLR2). Comb3 with a fixed coastline reduced warming effect, decreasing temperature by ~ 0.5 to 1 °C in summer relative to the Warm, but enhanced temperature PVD up to 1.5 °C in summer. Comb2 (Comb1 similarly) incured a warmer bay, warming up to 3-5°C (Table1, Figure 2, and Figure 3).

Experimental results on salinity and its PVD

The salinity of the bay changed radically for the cases that widen the geometry (i.e., SLR1, SLR2, Comb1, Comb2, SLR2I, SLR2W, SLR2WD, and Comb2WD). SLR2 and Comb2 had similar effects on salinity and temperature with SLR1 and Comb1 and were used as the representative cases for SLR and SLR under comprehensive conditions.

Relative to the Norm and based on standard cases, salinity and its PVD changed with cases. The Comb2 (Comb1 similarly) and SLR2 (SLR1 similarly) increased the mean salinity by 6 to 12psu (or from 1 to 17psu from the mouth to the upper bay), and decreased salinity PSV up to 4psu (0.6psu averaged yearly, ~0.8 to 0.9psu averaged during spring and summer, and by ~0.3 to 0.4psu averaged during the winter and fall). At the contemporary salt wedge location (30-80 km from the mouth), the salinity departure from the Norm was ~5 to 17psu (larger during the spring and summer when river discharge was seasonally stronger than during winter and fall). The HC1 reduced salinity up to 3 and increased salinity PVD up to 1 if without SLR, but slightly reduced salinity if with SLR2. The Comb3 kept salinity from increasing much, but intensified the salinity PVD by ~0.5psu (Table 1, Fig.2, and Fig. 3).

The salt-intrusion distance (SID) is employed here to evaluate horizontal salinity structure.

The SID is the function of freshwater input rates (Qriv, m3/s), as

$$SID = pQriv^{q} \quad (1)$$

The parameter q can represent the salinity sensitivity to river flow input rate. q = -1/3, implying that the SID (therefore, salinity) is relatively sensitive to river discharge input [16, 29, 30]. Within Delaware Bay, $q \approx$ -0.1 to -0.16, the SID is less sensitive to river discharge input, depending on isohalines based on idealized ROMS simulations using a constant river discharge and M_2 and S_2 tidal constituents [17].

This study used river discharge inputs from six rivers and seven tidal constituents (M_2, N_2, S_2, K_1, O_1, M_4, and M_6) [4]. If without SLR within the entire three-year period, q = -0.054 to -0.264 with tidal signals included; q= -0.041 to -0.277 without tidal signals included. A similar result was produced for isohalines 12.5, 15, 17.5, and 25psu. The parameter q was solved via the least-squared regression for the SID and river flow input rate (more data were listed in Table 2, and the SID was depicted in Figure 4). Without the SLR, the SID and salinity were sensitive to river discharge input, with the SID delaying river discharge input by a couple of weeks, and with the RD1 decreasing the mean salinity (18.2psu) by ~1.6psu. If with SLR2 within the entire three-year period, q = -0.0001 to -0.0156 with tidal signals included; q = -0.0001 to -0.145 without tidal signals included. The SID and salinity were much less sensitive to the river discharge input rate within the new enlarged and salinized bay, with the RD1 decreasing the mean salinity (26.2psu) by approximately 0.5psu (the SLR2 versus the Comb2).

Under contemporary conditions, salinity over much of the bay was considerably lower than the oceanic salinity and changed sensitively with river discharge, with a salt wedge localized at mid-bay. However, a 50-100 cm SLR incurred a bay of much higher salinities that responded insensitively to river flow input, with the salt wedge disappearing, and with the along-bay salinity gradient reducing from ~31.9 (during Norm) to ~7.2 ($\times 10^{-5}$ psu/m, also see Fig. 9), "salinizing" the bay. In order to quantitatively evaluate estuarine salinization, here developed a new experimental index, "estuarine salinization index (ESI, %)", that was defined as the percent of the net salty area (the area of the bottom water whose salinity is higher than 17.5psu) relative to total water area

$$ESI \equiv 100 \times \frac{\Delta A_S - \Delta A}{A} \qquad (2)$$

Where, ΔA_s and ΔA are the increments (m^2) of salty-water and water areas, respectively.

Positive/negative ESI indicates salinization/desalinization with a net salty-water area increment. The larger the ESI, the more an estuary is salinized. As listed in Table 1, the ESI was ~23% during SLR2. During the RD1, a slight desalination was induced from April to November, with the ESI of -8%. Intensified river discharge during the Comb1/Comb2 did not help reduce the salinization induced by the SLR1/SLR2, with the ESI of 22%/21%. During case SLR3/Comb3, a 100-cm SLR would not cause serious salinization with the ESI of 7%/4%.

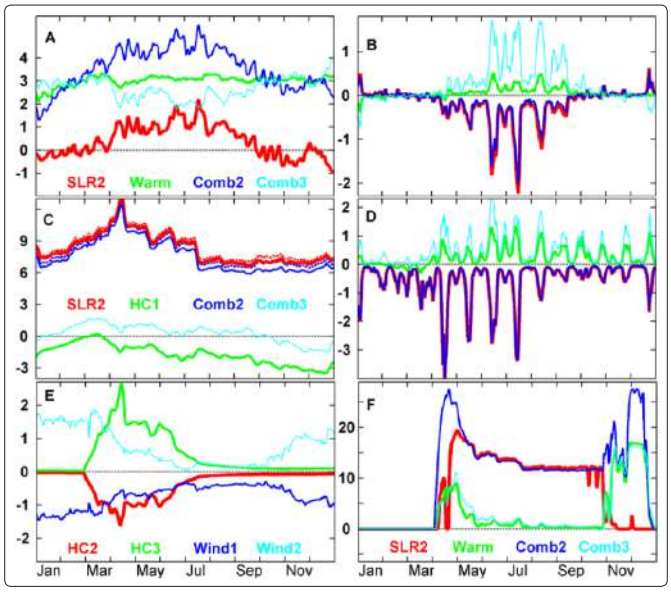

Figure 2: Departures of bottom temperature (°C, A) and temperature PVD (B), bottom salinity (psu, C and E) and salinity PVD (psu, D), and salty-warm water area (SWA, x100 km^2, F), based on simulation in one year after the model runs through the first year for full adjustment. Salinities, temperatures, and their PVD are all averaged within Delaware Bay with/without sea level rise. Dashed lines in C indicate the salinity and its PVD for SLR2 and Comb2, and are averaged within the bathymetry without sea level rise.

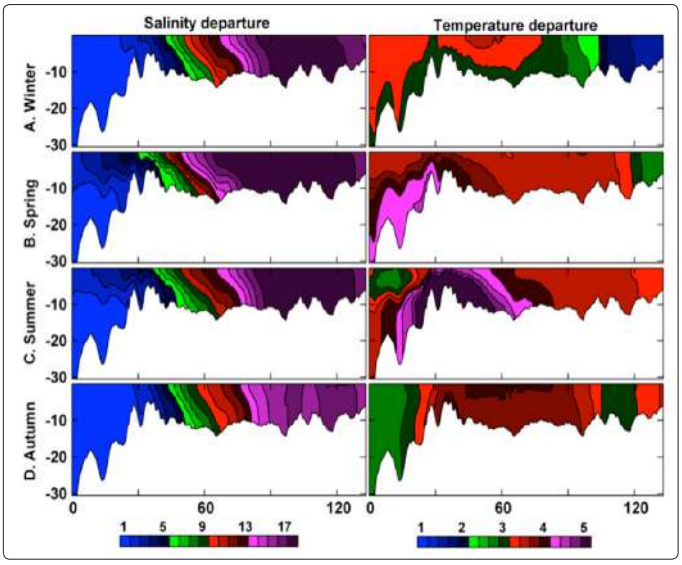

Figure 3: Seasonal departures of Comb2 from Norm of salinities (psu) and temperatures (°C) along the bay: The x-axis is river distance (km), and y-axis is depth (m).

Table 2: Salinity sensitivity to river flow input in Delaware Bay, expressed with parameter q as defined in Equation 1 and solved via least-squared regression for the SID and river flow input rate. p is the fitting coefficient. Norm and SLR2 use the same sample size of 15,989 in space and 17,520 in time within the three-year period.

Parameter		q [× (−1000)]				p (km)			
Isohalines		12.5	15	17.5	25	12.5	15	17.5	25
Tide	Norm	138±20	108±54	112±15	220±44	140±22	104±47	93±12	95±11
	SLR2	0.1±0	23±15	92±10	153±6	112±4	126±6	178±3	135±11
No tide	Norm	146±23	96±55	111±15	231±47	146±24	96±47	93±12	99±14
	SLR2	0.1±0	22±14	88±12	145±3	112±4	127±6	174±6	129±11

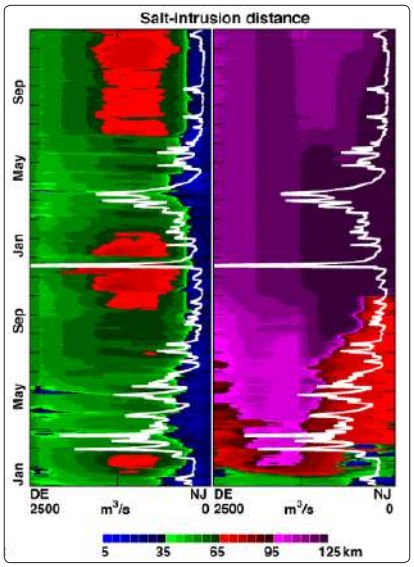

Figure 4: Time series of salt-intrusion distance (SID, contour) for the 17.5psu-isohaline (x-axis from Delaware-DE to New Jersey-NJ sides) and the river discharge (white curve) for cases Norm (left) and SLR2 (right), based on modeling.

Further experiments for salinity sensitivity were performed based on diagnostic cases. The SLR1 and SLR2, or the Comb1 and Comb2 produced an identical effect on salinity, implying that a widened geometry of the bay matters more in increasing salinity than the deepened depth of the bay for a 50 to 100-cm SLR, which was further confirmed by a case SLR2W whose mean salinity was only slightly lower (by ~1.9 psu) than the mean salinity of SLR2. The validated model used a 2-meter minimum depth for all standard cases.

Will a smaller minimum depth make difference in changing salinity? As compared to case SLR2 and averaged within a three-year period within the entire Delaware Bay, case SLR2WD induced a lower salinity, by ~0.8 psu, the RD1 decreased the mean salinity by ~1.4 psu (cases SLR2WD versus Comb2WD), and SLR2WD still incurred salinization of the bay with the mean salinity increasing by ~7.7 psu (cases SLR2WD versus NormWD) as the SLR2 did with the mean salinity increasing by ~8.5 psu (cases SLR2 versus Norm).

The fresher initial condition in case SLR2I provided a larger salinity contrast between the salinity within Delaware Bay and in the open ocean at the beginning. Little difference in salinity during the SLR2I was made as compared to the case SLR2, ~0.7 psu if averaged within the first two years. As compared to the standard cases, the diagnostic cases made little difference in changing salinity and had approximately the same results as the standard cases (Fig. 5).

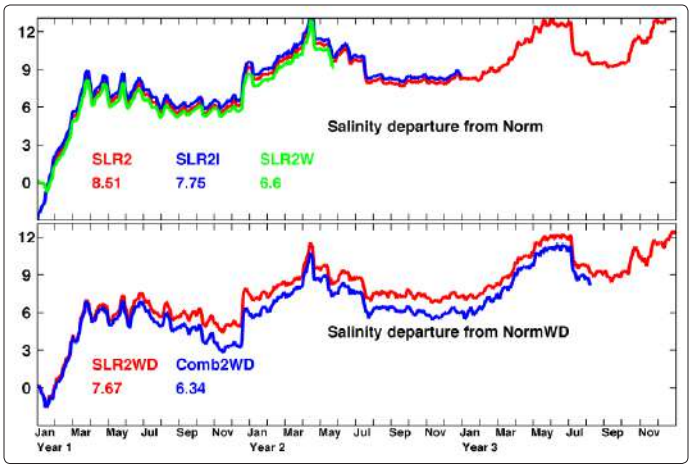

Figure 5: Salinity departures (psu) from case Norm for cases SLR2, SLRI and SLR2W (above), and from case NormWD (below), based on the salinity averaged within entire Delaware Bay.

4. Potential impact of the new physical conditions on oyster abundance

Two fatal diseases, MSX and Dermo, multiply faster at higher temperature (above 18-20°C) and salinity higher than approximately 12psu [2, 9]. A warm and salty environment (quantified with SWA that positively correlated to the MXSP) rarely occurred with the out-of-phase salinity and temperature via temperature-regulated river discharge. However, the warming climate and SLR incurred a warm and salty Delaware Bay with a larger SWA. The major contribution to increasing SWA was salinity during spring-summer-fall when the bay was warmer than 12.5°C, and was temperature at the lower bay during spring and fall when temperature could be lower than 12.5°C (see Figure 2F). Therefore, SLR (e.g., SLR2) that changed salinity the most and Warm that changed temperature the most, as well as their combinations (the Comb1 and Comb2), mainly influenced the SWA.

As shown in Figure 6, the SLR2 increased the SWA (normally ~770 km^2) by ~38%, Comb2 by ~75%, Warm by ~37%, SLR3 by ~10%, while RD1 reduced SWA by ~12%. Normally, the oyster beds were located near the border of the salty-warm water. SLR or SLR plus Warm caused the salty-warm water to cover all of the oyster beds. In the regular case, the spring salinity surrounding Egg Island, New Bed, and Bennies was below 17.5psu, the salinity surrounding Cohansey and Arnolds was always below 17.5psu, and the spring temperature surrounding all the oyster beds (including Leased Grounds) was below 12.5°C. SLR2 made the salinity surrounding all of the oyster beds higher than 17.5psu and made the summer-fall temperatures surrounding all of the oyster beds higher than 12.5°C. SLR2 plus Warm made the temperatures surrounding all of the oyster beds always higher than 12.5°C.

Therefore, the potential climate changes in SLR and temperature might be fatal to oysters via promoting MSX and Dermo diseasies in Delaware Bay.

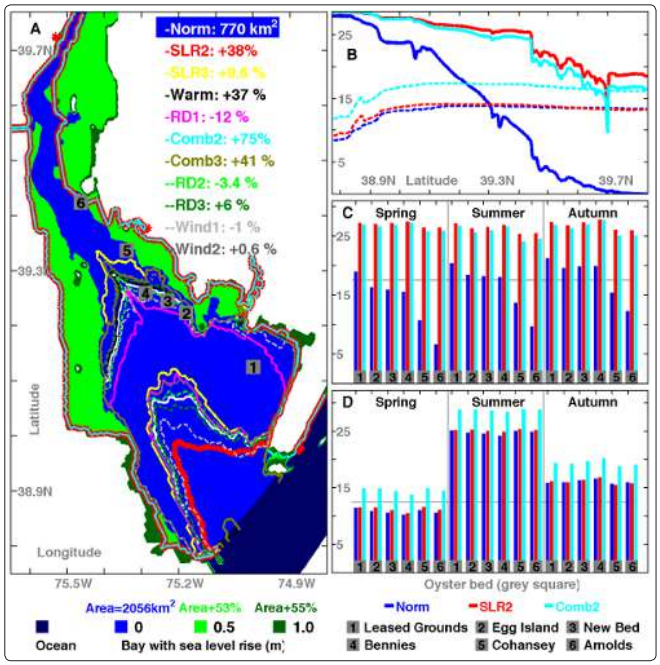

Figure 6: Mean SWA, salinity (psu) and temperature (°C) within the equilibrium phase: **A**. SWA (km^2) within the color contours for the listed eleven cases (as described in Table 6-6). The color regions indicate the ocean and the bay with SLRs. **B**. Along-bay salinity (solid lines) and temperature (dashed lines). **C/D** Seasonally averaged bottom salinity/temperature surrounding the oyster beds. Color scheme: Norm-blue, SLR2-red, and Comb2-cyan. The gray squares indicate oyster beds.

5. Theoretical consideration: Geometry or bathymetry that matters more to salinity

SLR induced an intensified SID

Assuming that the only mechanism responsible for the down-gradient salt flux is the steady shear dispersion, the SID is summarized elegantly as [16, 29 30].

$$SID = 0.024H^{8/3} \times \sqrt[3]{\frac{A\, g^2\, \beta^2\, S_{in}^2}{Q_{riv}\, K_M^2\, K_q}} \qquad (3)$$

Where H and A are the depth (m) and cross-sectional area (m^2) at the estuary mouth, respectively. Q_{riv} is river input rate (m^3/s), S_{in} the salinity of inflow from the ocean; g≈ 9.8m/s^2 (the Earth's gravitational constant), β ≈ 7.7×10^{-4} (the density-change rate with salinity), and K_M/K_q the eddy viscosity/diffusivity (m^2 s^{-1}).

Equation 3 partially explains the SID that increases with the water depth, the cross-sectional area, and salinity, but decreases with the eddy viscosity and diffusivity. The SLR1 increases the depth/cross-sectional area of Delaware Bay by approximately 10%/14%, with the other parameters fixed, the SID should be increased by approximately 35%. However, this estimation was much smaller than the modeling results: The SID of the 17.5-isohaline in SLR2 intruded approximately 110% that in the Norm. Equation 3 explains only approximately 32% the SID due to the following reasons:

1. Equation 3 is based on the steady shear dispersion that is approximately 17% of the summed mean salt fluxes (~12927 kg/s) from advection (~8206 kg/s), steady shear dispersion (~2189 kg/s), and tidal oscillation (~2522 kg/s) at the mouth in the SLR2-Norm difference. For Delaware Bay, steady shear dispersion was not the only major term for the salt flux. The advective and the tidal oscillatory salt fluxes also contribute by~ 63% and ~ 20% to the summed mean salt fluxes. The total salt flux was not zero (~ 3495 kg/s) during adjustment phase (Fig. 7).
2. The bathymetry and geometry of Delaware Bay vary greatly. The SLR enlarged the depth and cross-sectional area mainly within the middle and upper bay where their original values were relatively small, which should enlarge the SID further from the view implied in Equation 3. If the "Mouth" were located at an upper place, the theoretical estimation would be larger.
3. Finally, the SID decreased with eddy viscosity and diffusivity at the mouth in Equation 3. However, enhanced mixing changed the structure of the salinity and therefore the salt flux, as shown in details below.

A wider bay facilitates the exchange of salt flux

An asymmetry existed in the salinity and SID with a larger SID and a higher salinity on New Jersey side than on the Delaware side. The asymmetry was bigger during the SLR2 than during the Norm. For the originally narrow middle and upper bay, the freshwater from the upper bay mainly directly met the saline oceanic water from the lower bay to hinder the intrusion of the saline oceanic water. However, in the SLR2-induced wider bay, the flows from the upper bay and from the lower bay slid by one another by respectively moving to the Delaware and New Jersey sides, especially under the Coriolis force (Figure 8).

The salt-ridge distance, defined as the cross-bay length between the left bank and the highest-salinity locations to locate the saltiest inflow from the ocean, can increased up to approximately 20 kilometers within the middle bay during the SLR2, as compared to during the Norm. Also, the wider bay induced by SLR2 may enhance the geotropic motion with a smaller Rossby number ($R_o = U/fL$, $f = 2\times7.292\times10^{-5}\times sin\varphi$ s^{-1}: R_o<0.1, the Coriolis force dominates, R_o>1, the Coriolis force is omittable, if the width of the bay is used as the horizontal scale L, R_o = 0.26 (0.04 ~ 0.50) during the Norm while Ro = 0.05 (0.01 ~ 0.16) during SLR2. The differences (SLR2 minus Norm) of the Rossby number correlated to salt-ridge distance with a correlation coefficient of -84% (confidence>95%, Fig. 9).

A widened bay enhanced mixing, changing the salinity structure and the salt flux

A Mellor-Yamada level 2.5 scheme and k-kl parameters were applied in the modeling [11, 12]. The mixing intensity can be scaled using the turbulent kinetic energy (TKE) [13]. With nearly the same geometry but a different bathymetry, the SLR1 and SLR2, or the Norm and SLR3 produced identical effects on salinity, implying that the geometry matter to the salinity field, according to the above experiments. The SLR (e.g., SLR2) substantially increased the width within the middle bay (30-80 km from the mouth) (by ~40 to 200%). The TKE increased by ~5 to 50% within the middle bay. During both the adjustment and equilibrium phases, the TKE difference was correlated to the width difference between the SLR2 and Norm along the bay, with a correlation coefficient of 84% at a confidence level above 95% using t-test (Figure 9). The TKE was larger in SLR2 than in Norm and this TKE difference highly (29%, confidence >95%) correlated to the salt flux difference between the SLR2 and Norm within the adjustment phase (Figure 10).

Mixing influenced the salt flux by changing salinity structure. Due to the increased mixing, the along-bay salinity gradient reduced from ~31.9 $\times10^{-5}$ psu/m during the Norm to ~7.2×10^{-5} psu/m during the SLR2 (Figure 9C). Consequently, the advective salt flux reduced with the weakened salinity gradient and kept more salt inside the bay. The advective salt flux was a major term in the salt flux budget (Figure 7) with the salt flux from the advective term ~90% correlated to the total salt flux, as diagnosed in follows:

At a cross-section on x-z plane with a total cross-sectional area A (m^2, its tidally averaged value is A_o=<A>, dA=dx dz for a cell), the along-channel current ($V=V_o+V_e+V_t$, m/s) was decomposed into the tidal current (V_t), the estuarine exchange flow (V_e, defined in Eq. 4 below), and the net outflow ($V_o=\frac{1}{A_o}<\iint v dA>$) due to river input. The salinity (S) was decomposed into the salinity parts (S_o, S_e, and S_t) accordingly for these current components with $S=S_o+S_e+S_t$ ($S_o=\frac{1}{A_o}<\iint S dA$, $S_e=\frac{<SdA>}{<dA>}-S_o$). The along-channel salt flux (F_s, kg/s, defined in Eq. 5 below) integrated at a cross-section was accordingly decomposed into a steady shear dispersion (F_e) that was associated with the exchange flow to bring salt into the bay, an advective term ($F_o=\frac{-\rho}{1000}Q_{riv}S_o$, ρ represents density, kg m^{-3}) that was associated with the river outflow to bring salt out of the bay, and a tidal oscillatory salt flux (F_t) that tended to bring salt into the bay due to the out-of-quadrature salinity and velocity fields.

$$V_e(x,z,t) = \frac{<VdA>}{<dA>} - V_o \quad (4)$$

$$\begin{aligned} F_s(t) &= \frac{\rho}{1000} < \iint_0^A V\,S\,dA > \\ &\approx \frac{\rho}{1000} < \iint_0^A (V_oS_o + V_eS_e + V_tS_t)\,dA > \\ &= F_o + F_e + F_t \end{aligned} \quad (5)$$

Brackets represent the sub-tidal low-pass Lanczos filter with a 32-hour cut-off period for the hourly averaged simulations [17]. The salt flux difference between the cross-sections at the mouth (designated as 1) and Arnolds (designated as 2) was used to estimated the net salt input into the major bay

$$\begin{aligned} dF_s(t) &= \frac{1}{1000}\left[\iint_0^{A_1} v_1 s_1 \rho_1\,dA_1 - \iint_0^{A_2} v_2 s_2 \rho_2\,dA_2\right] \\ &= dF0 + dFe + d\,Ft \end{aligned} \quad (6)$$

$$dF_0 = \frac{-1}{1000} Q_{riv}\ \rho\ (S_1 - S_2) \quad (7)$$

Intensified mixing induced by the SLR weakened along-bay salinity gradient with a smaller S_1-S_2 and, therefore produced a smaller advective salt flux. During the adjustment phase, the SLR2-bay gains more salt flux (approximately 8,206 kg/s) than in the Norm at the mouth via the advective term. After being balanced by shear dispersion (approximately -2,189 kg/s) and tidal oscillation (approximately -2,522 kg/s), approximately 3,495 kg/s more salt flux was input into the bay, increasing the mean salinity by ~7.2psu within one year. Net salt flux input into the bay between the mouth and Arnolds was ~ 3,550 kg/s, increasing the mean salinity by ~ 7.4psu within one year. During the equilibrium phase, the net salt flux input to the bay between the mouth and Arnolds was ~ 989 kg/s, increasing the mean salinity by ~ 2psu within one year (Fig. 7 and Fig. 10). After the bay became fully mixed, a reduction in net salt flux was due to the reduced cross-bay salinity gradient, and can be explained by using Eq. 5, which could be re-written as follows:

$$F_s(t) = \frac{\rho}{1000}\left[\iint_0^{A^{in}} v\ s\ dA + \iint_0^{A^{out}} v\ s\ dA\right]$$
$$\approx \frac{\rho}{1000}\left[V_{in}(S_{in} - S_{out}) + S_{out} Q_{riv}\right] \quad (8)$$

Where, $A = A^{in} + A^{out}$. A^{in} and A^{out} are the integrated cross-sectional area when $v > 0$ and $v < 0$, and S_{in} and S_{out} the areal mean salinity of inflow and outflow, respectively.

On average, a cross-bay salinity-gradient existed on the cross-section at the mouth (Figure 10), with the salinity changing from approximately 27.5 to 24.5psu. The outflow was located at the upper layer near the area between two flanks while the inflow took a lower layer during the Norm, maintaining the salt exchange. In the well-mixed bay during the SLR2, the cross-bay salinity-gradient was weakened, ~28-25.6psu in the adjustment phase, and was further reduced to 28.4-27.4psu in the equilibrium phase, resulting in an inflow and outflow salinity difference that is too small and to bring less salt into the bay ($S_{in} - S_{out}$ = 0.26~0.77psu during the Norm versus 0.50 ~ 0.05psu during the SLR2).

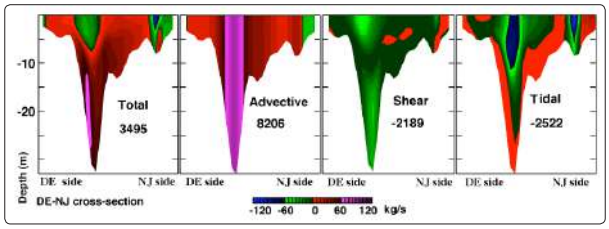

Figure 7: Salt flux difference form case Norm for the total, advective, shear-dispersion, and tidal terms (frames from left to right), averaged at the mouth within year 1 (area-integrated salt flux difference numbered and printed within the frames).

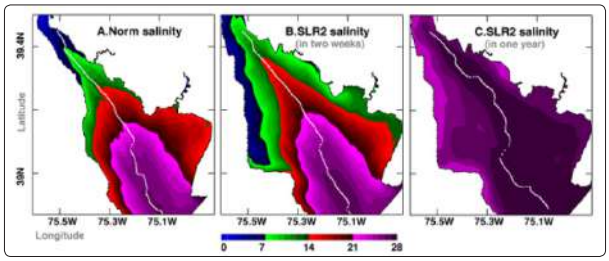

Figure 8: Vertically averaged salinity (psu) for Norm after model running for one year (A) and for SLR2 after model running for two weeks (B) and one year (C).

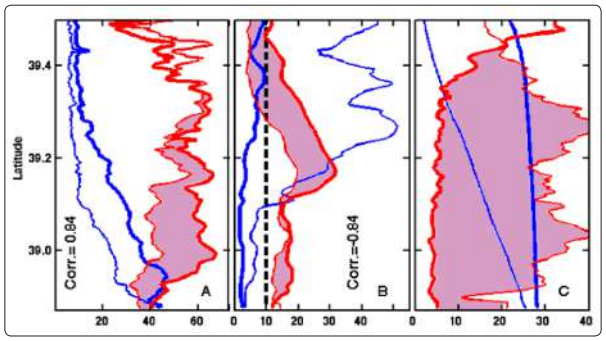

Figure 9: A: Along-bay geometric width (blue, km) and TKE (red, $\times 10^{-5} m^2/s^2$) for Norm (thin curves) and SLR2 (thick curves), with correlation 0.84 in the differences between SLR2 and Norm. **B**: Rossby number (blue, $\times 10^{-1}$) and salt-ridge distance (red, km) for Norm (thin curves) and SLR2 (thick curves), with correlation 0.84 in the differences between SLR2 and Norm. **C**: Salinity (blue, psu) and its along-bay gradient (red, $\times 10^{-5}$psu/m) for Norm (thin curves) and SLR2 (thick curves).

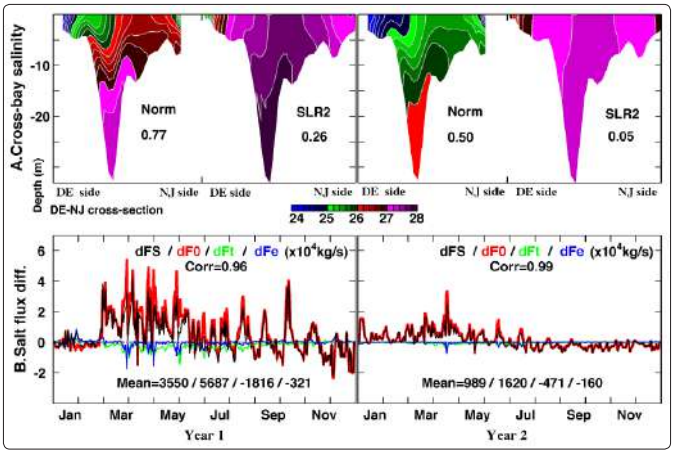

Figure 10: A Cross-bay salinity (psu) averaged at the mouth as defined in Eq. 6-31 (mean S_{in}-S_{out} numbered). **B**. *dFs*, *dF0*, d*Ft* and d*Fe* (see text). *dFs* correlates to dF0 (0.96/0.99, confidence>99%) and to TKE difference within adjustment phase (29%, confidence>95%, with TKE leading 42 days)

Summary and discussion

Estuaries may be sensitive to climate changes in their physical environment and related ecosystems. Eighteen numerical experiments were carried out to explore the potential impacts on the physical environment of Delaware Bay from the climate changes in sea levels, sea-surface air temperature, hydrological conditions, and sea-surface winds. The sensitivity experiments suggest that Delaware Bay may be vulnerable to a 50-100-cm SLR that may enlarge the size (width, depth and volume) of the bay. A 50-100-cm SLR may intensify mixing to weaken the along-bay horizontal salinity gradient mainly via widening the bay from a narrow "pipe" into a wider "pool", and may introduce more salt (160-190 million tons) into the bay until the equilibrium where the fully mixed salinity limited more salt from intruding into the bay, as summarized in Figure 11.

The comparison among the SLR cases showed that wider geometry mattered to estuary salinization more than a deeper bathymetry did

with a 50-100cm SLR. The SLR-induced salinization might not be offset by the intensified hydrological condition with river flow increasing 20 to 200% because salinity would be much higher and less sensitive to river flow input. However, a fixed coastline would substantially mitigate the salinization induced by the SLR. The missed salinity gradient due to SLR-induced estuary salinization would negatively affect the ecological system of Delaware Bay. The habitable and freshwater area would reduce with the intensified mixing and weakened salinity gradient. With the SLR plus warmer sea surface air, a salty-warm environment would be dominant within Delaware Bay and be unfavorable to oysters because MSX and Dermo diseases might multiply fast under such a salty-warm environment. The habitable and freshwater area would reduce with the intensified mixing and weakened salinity gradient.

The low-lying areas neighboring the bay leave the bay susceptible to sea-level rise with the area of the bay increasing rapidly with a 50-cm SLR (Figure6-4); on the other hand, low (including neap) tides did not incur a narrower geometry most of time according to the experiment from the SLR2WD performed for a three-year period, with experimental results depicted in Figure 12.

Tidal heights, averaged within entire bay with maximum amplitude of ~0.55 cm, were less than -0.25 cm during approximately 23.4% time and the wet area reduced only by 2%, with the width reducing little. Most (76.6%) of the time, the averaged tidal heights were higher than -0.25 cm, causing only 1% drying area. The TKE generally reduced with narrowed bathymetry from lower to higher bay. Stronger TKE was also produced at higher bay when the averaged tidal heights were lower than -0.25 cm, with the spring tides included. When the amplitudes of the averaged tidal heights were higher than 0.3 cm (~0.9% in time) or lower than -0.3 cm (~0.2% in time), the TKE became stronger due to the spring tides. The smaller amplitudes (-0.15 – 0.15cm, ~29.6% in time) with neap tides included may incur a stronger TKE in the lower bay, as compared to the averaged TKE for averaged tidal heights that were higher than -0.25 cm. The TKE correlated to the salt flux from steady-shear dispersion plus tidal oscillation (correlation=68%, confidence >95%, based on 1096 daily average samples), implying that stronger mixings cause stronger salt fluxes into the bay via steady- shear dispersion plus tidal oscillation.

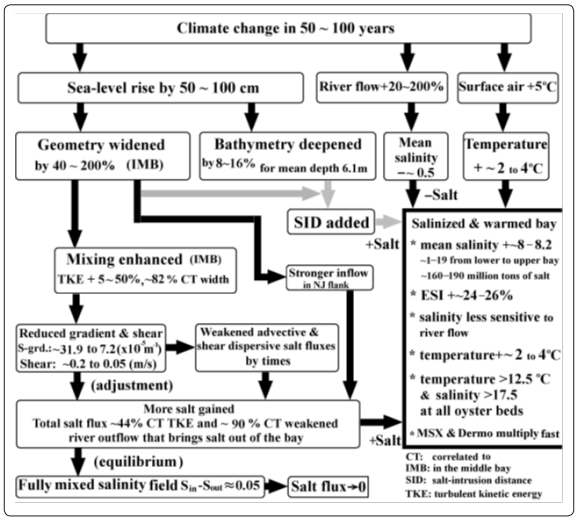

Figure 11: Schematic of the salinized and warmed Delaware Bay: The gray arrows indicate a relationship without having been quantitatively experimented on in this study

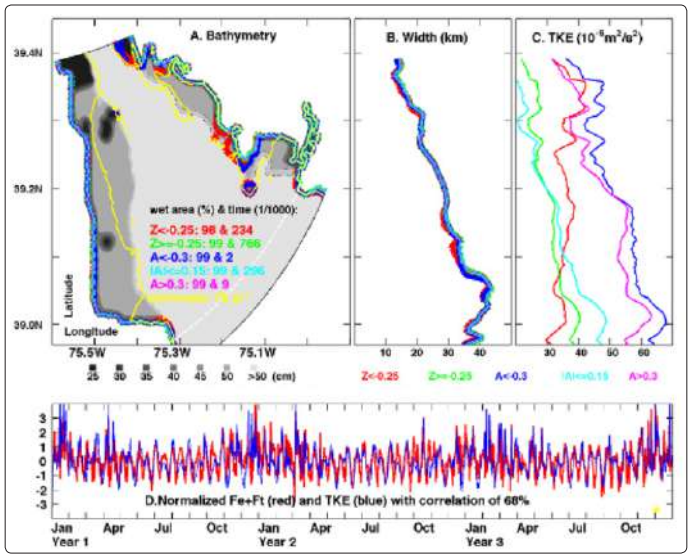

Figure 12: Bathymetry, tides, mixing and salt-fluxes during case SLR2WD using wet-dry scheme with coastline changing with each time step (15 seconds) and with a 25cm minimum depth. **A**. Bathymetry versus wet area circled by color curves for different tidal heights (Z) and its amplitude (A) averaged within the entire bay. **B/C**. Width/TKE averaged along the bay. **D**. Daily averaged normalized TKE (blue) and the steady-shear-dispersion (F_e) plus tidal oscillatory salt flux (F_t) via the cross-section near the mouth indicated by the white dashed line in A. Correlation between the TKE and *Fe+Ft* was computed using 1096 daily samples averaged within the entire domain of A. The "*" is the time point for the minimum wet area.

Other similar estuaries may be salinized with the SLR. Based on the availability of high-resolution topography, seventeen such estuaries including thirty-five bays were selected along the U.S. coast (Table 3). They (e.g., Baffin, Copano, Mud, Albemarle, and Chesapeake) have shallow depths (mean depth<7 meters, maximum depth ~113m for Chesapeake Bay), small volumes (<7.6 km^3) except Chesapeake Bay (~67 km^3), and narrow geometries. A 50-100 cm SLR will substantially widen their geometries, deepen their depths (>14% of their mean depths), enlarge their volumes (19% for Chesapeake Bay, >35% for others, partially shown in Fig.13), and could salinize them. However, the studies based on more data and experiments should be 538 performed prior to such claims evaluate the extent on which those estuaries might be salinized.

Table 3: Sea-level rises and the sizes of the estuaries picked along the U.S. coast. Seventeen estuaries 539 including thirty-five bays were selected along the U.S. coast where high-resolution topography are available based on gridded 3-second database provided by the National Geophysical Data Center (NGDC) U.S. Coastal Relief Model. Global gridded 2-minute database from the NGDC U.S. Department of Commerce are also applied here to compute the size of global water and land.

Estuaries along U.S. coast	SLR = 0			SLR = 0.5 m		SLR = 1 m		SLR = 2 m		SLR = 3 m	
	Depth (m) Max/mean	Vol. 10^9 m^3	Area 10^9 m^2	Vol. +%	Area +%	Vol. +%	Area +%	Vol. +%	Area +%	Vol. +%	Area +%
A. North	12.5/0.7	0.16	0.218	69	2	141	12	294	15	454	19
B. Willapa	19.0/2.1	0.77	0.367	24	2	49	6	100	11	154	17
C. Tillamook	0.9/0.2	0.01	0.037	222	7	459	26	103	46	1685	61
D. Coos	6.3/0.2	0.01	0.043	246	12	518	23	113	39	1819	56
E. Arcata[e+]	0.1/0.1	0.01	0.067	533	10	1120	60	285	94	4941	139
F.San Pablo[f+]	87.4/2.4	6.05	2.533	21	7	44	28	99	50	163	65
G. Baffin[g+]	2.9/1.3	0.26	0.203	39	7	81	32	186	54	309	112
H. Copano[h+]	5.9/1.3	0.90	0.716	40	3	82	23	181	49	304	86
I. Lavaca[i+]	12.5/1.1	0.33	0.293	45	4	92	21	202	45	336	123
j.Galveston[j+]	16.0/1.5	1.87	1.266	34	2	69	18	149	27	235	39
K.Tampa[k+]	15.7/2.8	3.19	1.145	18	3	37	8	76	35	126	59
L. Mud[l+]	17.1/1.2	0.19	0.158	41	6	85	22	188	54	319	127
M. Buzzard	14.2/1.5	0.17	0.119	35	12	74	28	166	52	273	74
N. Stones	5.3/1.4	0.13	0.099	38	8	79	17	170	39	278	57
O. Albemarle	13.1/1.6	7.56	4.879	32	2	65	20	144	39	234	74
P.Chesapeake	112.7/6.3	73.61	11.67	10	34	21	35	43	40	66	45
Q. Delaware	46.7/6.4	13.19	2.056	12	53	24	55	49	63	75	72
Area change of global water (+) and land (-)		km^2		140,740		232,750		2,447,600		2,763,300	
		% (*)		0.0276		0.0456		0.4799		0.5418	

e+, Humboldt and South; f+, San Rafeel and San Francisco; g+, Alazan; h+, Mission and Port; i+, Cox, Keller, Chocolate and Carancahua; j+, Trinity and East; k+, Hillsborough, East, McKay and Terra Ceia; l+, Winyah. * relative to total area 361,320,000 (water area) +148,740,000 (land area) km^2.

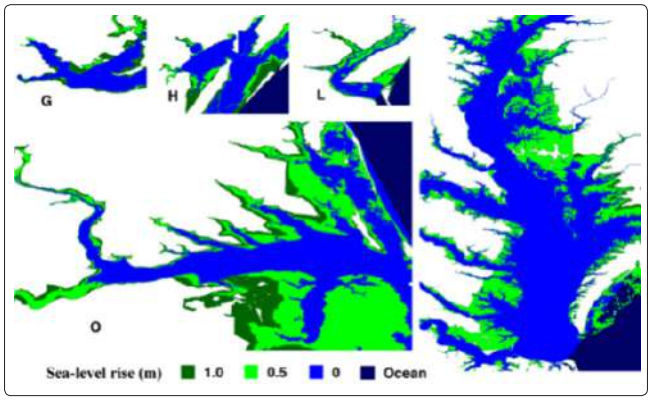

Figure 13: SLRs and water areas of estuaries **G**, **H**, **L**, **O** and **P** (Table 3), using gridded 3-second database from National Geophysical Data Center U.S. Coastal Relief Model.

Acknowledgements

Summarized and improved from my PhD thesis, this study has been supported by National Science Foundation Ecology of Infectious Diseases program (OCE06-22672). Funding was also provided by the Army Corps of Engineers under their Section 22 funding authority, contract #W912BU-11-C-0004, through the Seaboard Fisheries Institute. I was supported with Fellowship from the DuPont Corporation and the New Jersey Agricultural Experiment Station, advised by Dr. Dale Haidvogel, James Miller, Robert Chant, John Wilkin, Mark Miller, and David Bushek "(Institute of Marine and Coastal Sciences and Environmental Department, Rutgers University)". Data are from Delaware Bay Mooring Deployment Project, the Pre-Construction Oyster and Water Quality Monitoring Study for the Main Channel Deepening Project, the Ecology of Infectious Diseases program, the Delaware Environmental Observation System, the North American Regional Reanalysis and the European Centre for Medium-Range Weather Forecasting, the US Geological Survey for river discharge, the National Water Level Program for sea level height, the Global Advanced Circulation Model, and the National Geophysical Data Center | U.S. Coastal Relief Model "Dr. Robert Chant provided the salinity, temperature, and current data in 2010-2011 from the Delaware Bay Mooring Deployment Project-DBMDP. Drs. Eileen Hofmann (Department of Ocean, Earth and Atmospheric Sciences, Old Dominion University), David Bushek, Eric Powell, Susan Ford, and Jason Morson (Haskin Shellfish Research Laboratory, Rutgers University), and Principal Hal Brundage (Environmental Research and Consulting, Inc.) all provided supports including access to the Versar temperature and salinity in 2000 and MSX prevalence observations in 1958-2009. Drs. Kevin Brinson and Daniel Leathers (University of Delaware) provided the solar radiation from the Delaware Environmental Observation System." Research computing specialist Elias Hunter, computer experts David Robertson, Chuck Belmonte, and Adam Porter, and PhD Candidate Greg Seroka (Institute of Marine and Coastal Sciences, Rutgers University) are always helpful in facilities.

References

1. Haskin H H, L A Stauber, J A Mackin (1966) Minchinia nelsoni n. sp. (Haplosporida, Haplosporidiidae): causative agent of Delaware Bay oyster epizootic. Science 153: 1414-1416.
2. Ford S E and M R Tripp (1996) Disease and Defense Mechanisms. The Eastern Oyster: Crassostrea virginica. Maryland Sea Grant College, College Park, Maryland pp. 383-450.
3. Powell E N, A A Kathryn, J N Kraeuter, S E Ford, D Bushek (2008) Long-term trends in oyster population dynamics in Delaware Bay: regime shifts and response to disease. J. of Shellfish Research, 27: 729-755.
4. Wang Z (2014) Modeling of the Physical Environment and Its Effect in Delaware Bay, Verlag/Publisher: Scholars' Press, ISBN 978-3-639-70994-0 pp132.
5. Wang Z, D Haidvogel, D Bushek, S Ford, E Hofmann et al. (2012A) Circulation and Water properties and Their Relationship to the Oyster Disease MSX in Delaware Bay, J. Marine Res., 70, 279-308, DOI: http://dx.doi.org/10.1357/002224012802851931.
6. Andrews J D (1966) Oyster mortality studies in Virginia V. Epizootiology of MSX, a protistan pathogen of oysters. Ecology 47:19-31.
7. Haskin H H and S E Ford (1982) Haplosporidium nelsoni (MSX) on Delaware Bay seed oyster beds: a host-parasite relationship along a salinity gradient. J. Invertebrate Pathology 40: 388-405.
8. Ford S E (1985) Effects of salinity on survival of MSX parasite Haplosporidium nelsoni (Haskin, Stauber, and Mackin) in oysters. J. Shellfish Res 5: 85-90.
9. Cook T, M Folli, J Klinck, S Ford, J Miller (1998) The Relationship Between Increasing Sea-surface Temperature and the Northward Spread of Perkinsus marinus (Dermo) Disease Epizootics in Oysters.Estuarine, Coastal and Shelf Science 46: 587-597.
10. Knauss JA (2005) An Introduction to Physical Oceanography, 2nd Ed., Waveland Press. Inc pp309.
11. Mellor G L and T Yamada (1974) A hierarchy of turbulence closure models for planetary boundary layers. J. Atmos. Sci 31: 1791-1806.
12. Mellor G L and T Yamada (1982) Development of a turbulent closure model for geophysical fluid problems. Reviews of Geophysics and Space Physics 20: 851-875.
13. Umlauf L and H Burchard (2003) A generic length-scale equation for geophysical turbulence models, J.Mar.Res 61: 235-265.
14. Warner J C, C R Sherwood, H G Arango, R P Signell (2005A) Performance of four turbulence closure methods implemented using a generic length scale method, Ocean Modelling 8: 81-113.
15. Ralston D K, W R Geyer, J A Lerczak (2008) Subtidal salinity and velocity in the hudson river estuary: observations and modeling. J. Phys. Oceanogr 38 753-770.
16. MacCready P and W R Geyer (2010) Advances in Estuarine Physics. Annu. Rev. Mar. Sci 2: 35-58.
17. Aristizabal M, R Chant (2013) A Numerical Study of Salt Fluxes in Delaware Bay Estuary. J. Phys. Oceanogr DOI: 10.1175/JPO-D-12-0124.1
18. Nguyen A D (2008) Salt Intrusion, Tides and Mixing in Multi-channel Estuaries, Taylor & Francis/Balkema (PO Box 447, 2300 AK Leiden, The Netherlands) 174pp.
19. Chen M, P Xie, J E Janowiak (2002) Global land precipitation: a 50-yr monthly analysis based on gauge observations. J. Hydrometeorl 3: 249-266.
20. Wang Z, D Wu, X Chen, R Qiao (2012B) ENSO Indices and Analysis, Adv. in Atmosph. Sci 30 : 1491-1506.
21. Trenberth K E, P D Jones, P Ambenje, R Bojariu, D Easterling et al. (2007) Observations: Surface and Atmospheric Climate Change. In: Climate Change 2007: The Physical Science Basis. Contribution of Working Group I to the Fourth Assessment Report of the Inter governmental Panel on Climate United Kingdom and New York, NY, USA.
22. Najjar R G, L Patterson, S Graham (2009) Climate simulations of major estuarine watersheds in the Mid-Atlantic region of the US. Climate Change 95: 139-168.
23. Najjar R G, C P Pyke, M B Adams, D Breitburg, C Hershner (2010) Potential climate-change impacts on the Chesapeake Bay. Estuarine, Coastal and Ahelf Science 86: 1-20.
24. Church J A, N J White (2006) A 20th century acceleration in global sea-level rise. Geophys. Res. Lett doi: 10.1029/2005GL024826.
25. Gornitz V (1995) A comparison between recent and late Holocene sea-level trends from eastern North America and other selected regions. J. Coastal Res 17: 287-297.
26. Rudolf B, H Hauschild, W Rueth, U Schneider (1994) Terrestrial precipitation analysis: Operational method and required density of point measurements. In: Global Precipitations and Climate Change NATO ASI Series I, 26, Springer Verlag, Berlin pp173-186.
27. Lemke P, J Pen, R B Alley, I Allison, J Carrasco (2007) Observations: Changes in Snow, Ice and Frozen Ground. In: Climate Change (2007) the Physical Science Basis. Contribution of Working Group I to the Fourth Assessment Report of the Intergovernmental Panel on Climate Change, Cambridge University Press, Cambridge, United Kingdom and New York, NY, USA.
28. McCabe G J, M A Ayers (1989) Hydrologic effects of climate change in the Delaware River Basin. Water Resour Bull 25: 1231-1242.
29. Hansen D V, M Rattray (1965) Gravitational circulation in straits and estuaries. J. Mar. Res 23: 104-122.
30. Monismith S G, W Kimmerer, J R Burau, M T Stecey (2002) Structure and flow-induced variability of subtidal salinity field in northern San Francisco bay. J. Phys. Oceanogr 32: 3003-3019.

Copyright: *©2019 Zhiren Wang. This is an open-access article distributed under the terms of the Creative Commons Attribution License, which permits unrestricted use, distribution, and reproduction in any medium, provided the original author and source are credited.*